# Coulomb interactions and the integer quantum Hall effect: Screening and transport

N. R. Cooper and J. T. Chalker

*Theoretical Physics, University of Oxford, 1 Keble Road, Oxford OX1 3NP, United Kingdom*

We examine the influence of Coulomb interactions on the integer quantum Hall effect in high-mobility, wide spacer-layer heterostructures. In these devices, the potential due to disorder is expected to be smooth on the scale of the spacer-layer thickness, which can be much larger than the magnetic length. Screening of this potential is accompanied by large fluctuations in electron density and has dramatic consequences. In particular, the screened potential can be pinned to the Fermi energy in regions of the sample, and these regions can percolate over a range of Landau-level filling fractions. We present a theory for transport that includes screening within the Thomas-Fermi approximation. Considering the Hall conductance as a function of filling fraction, we show that risers between quantized Hall plateaus acquire a finite width in the presence of Coulomb interactions. We also show that, under certain circumstances, current flows within the sample only along narrow strips, concentrated around particular contours of the equilibrium electron density.

## I. INTRODUCTION

Many aspects of the integer quantum Hall effect can be satisfactorily explained in terms of a single-particle picture.[1] Quantized Hall plateaus occur when the Fermi energy lies in a mobility gap of the single-particle density of states. Disorder plays an essential role in producing localized states between Landau bands, which pin the Fermi energy in a mobility gap over a range of magnetic field. In fact, it is commonly accepted that disorder localizes almost all single-particle states, with the result that bulk states at the Fermi level are extended only at one singular energy within each Landau band. Consequently, risers between Hall plateaus become infinitesimally narrow at zero temperature. This is most easily visualized in a percolation description, appropriate when the potential due to disorder is smooth.[2] If the magnetic length is much shorter than the length scale for disorder, electron states lie on contours of the disordered potential. These contours form closed loops (localized states), except at the single energy in each Landau level for which the associated contours percolate through the disordered potential-energy surface. Correspondingly, at fixed average Landau-level filling fraction, the sample divides locally into two kinds of regions: those where the highest occupied Landau level is locally full and those where it is locally empty.

Although this argument is based on a semiclassical description, the presence of quantum tunneling[3] does not seem to alter the most important qualitative feature: the existence of a single energy at which the localization length diverges. This idea has been successfully tested in experiments, using *low-mobility* samples.[4−6] The width (in field) of risers between Hall plateaus is indeed found to extrapolate towards zero at zero temperature.

Nevertheless, there are a number of phenomena which demonstrate the importance of interactions. In particular, the single-particle description cannot account for the experimentally observed filling-fraction dependence of the Landau-level width.[7,8] The explanation requires a discussion of electron-electron interactions and screening of disorder. Various approaches[9−15] have been used, all relying essentially on the principle that when the Fermi level is near the center of a Landau band, electrons are free to adjust their density and screening is good, whereas when it lies between bands, they cannot and screening is poor. Screening of disorder takes on a very different character according to whether the disordered potential varies rapidly or smoothly on the scale of the magnetic length. It is most dramatic in the second case, which occurs in high-mobility samples in which the two-dimensional electron gas is separated from ionized donors by a wide spacer layer. The real-space theory of screening developed by Luryi[10] and by Efros[12−15] provides an appealing treatment of just this situation. The percolation description summarized above must be revised, since the screened potential-energy surface is determined self-consistently with the electron distribution. Within the Thomas-Fermi approximation, appropriate for a smooth disordered potential, a third kind of region occurs in the sample,[10] in addition to the local areas of full and empty Landau level present in the noninteracting system. The new, "metallic" regions are ones in which the local electron density is between zero and that of the full Landau level. At zero temperature the potential is perfectly screened and pinned at the Fermi energy within metallic regions. In this revised percolation description, the step between two quantum Hall plateaus is again associated with the transition of the Fermi level from above the percolating energy contour of the *screened* potential to below it. The effect of interactions, however, is that *over a range of magnetic field* between these two extremes, a metallic region percolates through the sample and the Fermi level is an extended contour of the screened potential. It seems natural to associate this with a nonquantized Hall conductivity. One therefore expects[10,15] transitions between Hall plateaus to have a finite width in filling fraction, even in the low-temperature limit. The conduction mechanism in this metallic region is, however, rather un-

clear. In particular, there can be no equilibrium drift of cyclotron guiding centers in these regions, since the screened potential has zero gradient.

The purpose of this paper is to elucidate the transport mechanism within the framework of Thomas-Fermi screening theory. We find at zero temperature that the Hall resistance is not quantized when a metallic region percolates and that risers between Hall plateaus have finite width in filling fraction. Thus we expect the quantum Hall effect in a smooth, screened potential to be qualitatively different from that observed in low-mobility samples. Systematic measurements of the temperature-dependent width of transitions between Hall plateaus in high-mobility, wide spacer-layer samples would be of great interest to test this prediction.

We begin in Sec. II by discussing the disordered potential of high-mobility devices in which the screening theory that we use is applicable. In Sec. III we review this screening theory and calculate for a simple example the resultant electron-density distribution. The essential features of our transport theory, based on the Landauer-Büttiker formalism,[16] are presented in Sec. IV, where it is used to describe a simple device, without disorder and in which only one Landau level is occupied. Our conclusions at this stage apply only to mesoscopic samples, since (in the spirit of the Landauer-Büttiker approach) we have assumed that dissipation occurs only in the contacts, and not in the sample. To check the stability of our results, and to extend them to macroscopic samples, we next introduce phenomenologically a diagonal component to the local conductivity tensor. In Sec. V, these ideas are applied to the conductance of more realistic Hall samples, which are much larger than the disorder length scale and have more than one Landau level occupied. The presence of inelastic scattering introduces a new scale, the *dissipation length,* which depends on the equilibrium density distribution and the strength of inelastic scattering. For samples much smaller than the dissipation length, inelastic scattering may be neglected, and it is straightforward to determine the conductance of the device from the equilibrium density distribution. For samples much larger than the dissipation length, transport in the partially occupied Landau level is represented by a resistivity, similar to that in a model proposed by McEuen *et al.*[17] on empirical grounds. We discuss this resistivity and show that under certain conditions it is independent of the size of the diagonal component of the local conductivity.

While preparing this work for publication, we learned of closely related studies by Chklovskii, Matveev, and Shklovskii[18] and by Ruzin.[19] These authors focus on a rather different problem—the two-terminal conductance of a ballistic device—from the one treated here, but their approach has much in common with the present paper. Most important, our conclusions in Sec. IV about the potential distribution within a mesoscopic device are in agreement with those of Refs. 18 and 19.

## II. IMPURITY POTENTIAL

We are concerned in this paper with the transport properties of Hall devices characterized by long-range potential fluctuations. Such a potential is typical of high-quality modulation-doped heterostructures, in particular, GaAs/Al$_x$Ga$_{1-x}$As devices, in which the electrons lie at a clean interface and scattering is predominantly due to ionized donors separated from the two-dimensional electron gas by a thick spacer layer.

To see how a long-range potential arises in such devices, consider the case of a $\delta$ layer of ionized donors, a distance $d$ away from the plane of the electron gas. A fluctuation of wave vector $k$ in the density of the charged donors sets up an electrostatic potential proportional to $(\exp - kd)/k$ in the plane of the electron gas. As a result, short-wavelength fluctuations are exponentially damped and the random potential is smooth on a length scale $d$. It seems reasonable to assume that the positions of the ionized donor impurities are uncorrelated, in which case it has been shown[12] that the root mean square of the potential-energy fluctuation for an electron in the electron gas is

$$\sqrt{\langle W_B^2 \rangle} = \frac{e^2}{\epsilon \epsilon_0} \left[ \frac{n_D}{8\pi} \ln \left[ \frac{L}{d} \right] \right]^{1/2} , \qquad (2.1)$$

where $\epsilon$ is the relative permittivity, $n_D$ is the average real density of ionized donors (which is close to the density of the electron gas), and $L$ is the system size. With values of the system parameters appropriate for typical quantum Hall samples, this energy can be very large and may even exceed the spacing between Landau levels. The important simplifying feature, however, is that despite such large energy fluctuations, the root mean square of the potential-energy *gradient,*

$$\sqrt{\langle |\nabla W_B|^2 \rangle} = \left[ \frac{n_D}{32\pi} \right]^{1/2} \frac{e^2}{\epsilon \epsilon_0 d} , \qquad (2.2)$$

can be small compared to $\hbar \omega / l$, the ratio of the cyclotron energy to the magnetic length. In this case it is possible to neglect Landau-level coupling, so that *locally* the single-particle density of states is ideal, and the effect of the random potential is just to bend the Landau levels on a length scale larger than $d$.

Correlations in the positions of the ionized donors[12] reduce the amplitude of these fluctuations, but do not alter the qualitative picture. In subsequent sections we will consider a bare potential of the form described above, but for simplicity will assume that the amplitude of the fluctuations is less than the cyclotron energy, so that Landau levels do not overlap.

## III. EQUILIBRIUM BEHAVIOR OF AN INTERACTING 2DEG

### A. Introduction

Our treatment of linear response in quantum Hall systems takes account of electron-electron intractions within Thomas-Fermi screening theory. Thus we combine the Hartree approximation with the additional assumption that the length scale $d$ is much larger than the radius of cyclotron orbits at the Fermi energy. This simplification has been used in a series of papers by Efros.[12-15] The

equilibrium behavior of the full Hartree problem has been studied both analytically[20] and numerically[21,22] for potentials that are translationally invariant in one direction.

If $d \gg l$, then an area of size $d^2$, over which the potential is roughly constant, contains many electron states. In this case it is possible to describe the electron distribution in terms of a local electron number density, which is determined by the position of the chemical potential relative to the Landau bands at that point. If the amplitude of the bare potential fluctuations is not large enough to cause adjacent Landau bands to overlap, then in the bulk of the sample the chemical potential lies within a single band, and only the electrons in this partially filled level are free to adjust their density, all other levels being fully occupied or completely empty. The free energy of the system is a functional of the density of these electrons:

$$\mathcal{F}[n] = \int W_B(\mathbf{r})n(\mathbf{r})d^2\mathbf{r} + \frac{1}{2}\int n(\mathbf{r})I(\mathbf{r}-\mathbf{r}')n(\mathbf{r}')d^2\mathbf{r}\, d^2\mathbf{r}'$$

$$-\mu\int n(\mathbf{r})d^2\mathbf{r} - k_B T\int n(\mathbf{r})\ln\left[\frac{n_0-n(\mathbf{r})}{n(\mathbf{r})}\right]$$

$$-n_0\ln\left[\frac{n_0-n(\mathbf{r})}{n_0}\right]d^2\mathbf{r}\,,\qquad (3.1)$$

where $W_B(\mathbf{r})$ is the bare disorder potential energy, $I(\mathbf{r})$ is the interaction energy between two electrons separated by the vector $\mathbf{r}$ (which, neglecting the thickness of the two-dimensional electron gas (2DEG), is simply $e^2/4\pi\epsilon\epsilon_0|\mathbf{r}|$), $n_0 = eB/h$ is the Landau-level density, $k_B T$ is the thermal energy, and $\mu$ is the chemical potential.

Additional terms may be introduced in (3.1) to model nonideal behavior of the electron gas due to finite thickness effects[24] or electron correlations.[15] In the following, however, we ignore local many-body correlations and, specifically, the dependence of energy on density, characteristic of the fractional quantum Hall effect. This approximation should be justified at temperatures high compared with fractional-state energy gaps. Since gap energies are much smaller than the potential-energy fluctuations discussed in Sec. II, we simplify much of our presentation by setting $T=0$. The approach has been used recently[23] to calculate the positions and widths of edge states neglecting disorder. We concentrate, in contrast, on the bulk of the sample, where the Landau bands are bent only by the impurity potential.

Minimization of the free energy with respect to variations in the number density leads to a coupled pair of equations for the screening electron distribution $n_s(\mathbf{r})$ and screened potential $W_S(\mathbf{r})$:

$$n_s(\mathbf{r}) = \frac{n_0}{1+\exp\left[\dfrac{W_S(\mathbf{r})-\mu}{k_B T}\right]}\,,\qquad (3.2)$$

$$W_S(\mathbf{r}) = W_B(\mathbf{r}) + \int I(\mathbf{r}-\mathbf{r}')n_S(\mathbf{r}')d^2\mathbf{r}'\,.\qquad (3.3)$$

We shall restrict attention to the case $T=0$,[13] when the Fermi function is a sharp step and the problem becomes to divide the plane of the electron gas into regions of three types:

$$n_s(\mathbf{r})=0\,,\quad W_S(\mathbf{r})>\mu\quad(\text{``empty''})$$

$$n_s(\mathbf{r})=n_0\,,\quad W_S(\mathbf{r})<\mu\quad(\text{``full''})$$

$$0<n_s(\mathbf{r})<n_0\,,\quad W_S(\mathbf{r})=\mu\quad(\text{``metallic''})$$

with $W_S(\mathbf{r})$ depending on $n_S(\mathbf{r})$ according to Eq. (3.3).

In general, this self-consistent problem for the electron distribution must be solved numerically, but for the purpose of this paper it is sufficient to gain a qualitative understanding of how the electrons adjust to the presence of the disordered potential. In the noninteracting problem, the electron gas would be divided into *full* regions and *empty* regions with a sharp boundary at the intersection of the bare potential with the constant Fermi level. The presence of interactions introduces *metallic* regions which smooth the transitions between full and empty. We shall see that there are effectively two regimes of behavior: "interaction dominated," where the metallic regions are large, and "potential dominated," where the distribution is similar to that in the noninteracting case.

### B. Qualitative features of screening

The series of diagrams in Fig. 1 show how a weak potential is screened as a function of filling fraction. At first, electrons are confined to wells of the bare potential, arranged in such a way that in these areas the screened potential is flat and pinned to the Fermi level [Fig. 1(a)]. As more electrons are added, these regions grow, at first joining to form a percolating *metallic* region and eventually to cover the whole sample. This is the case of *perfect screening* where the electrons acquire a density modulation which exactly compensates for the bare potential, leaving the screened potential completely flat [Fig. 1(c)]. As the filling fraction increases further, the density modulation remains fixed, while the average density increases, until in some areas the density saturates at $n_0$ to form localized *full* regions, which grow in size and join [Fig. 1(d)] to finally cover the sample when the filling fraction of the level is 1 [Fig. 1(e)]. The bare potential is now unscreened as the full level is unable to adjust its density. The characteristic behavior of this *interaction-dominated* regime, therefore, is to have a range of filling fraction over which the metallic region covers the whole sample, with a density modulation that is a *linear* function of the applied bare potential. Linear screening arises from a nonlinear problem as long as the whole sample is metallic and $W_S(\mathbf{r})=\mu$, so that it is possible to neglect (3.2) and simply invert (3.3) to obtain $n_S(\mathbf{r})$. Clearly, this condition cannot be achieved if the electrons are unable to adjust their density sufficiently, that is, if the level is close enough to integer filling fraction that the perfect-screening density modulation would require the electron density to either be negative or larger than $n_0$ at any point in the two-dimensional electron gas. At these values of filling fraction, perfect screening fails[12] and the screening is necessarily nonlinear.

When potential fluctuations are strong, the Landau-level density may be too small to allow the modulation

necessary for perfect screening, even when the level is half-full on average. We demonstrate in Sec. III C that this occurs when the scale for the Coulomb force, $n_0 e^2 / 2\pi\epsilon\epsilon_0$, is smaller than the typical bare potential gradient $\sqrt{\langle |\nabla W_B|^2 \rangle}$, and disorder dominates interactions. It is shown in Fig. 2 how the electrons are distributed in this case. Full regions are formed over the minima of the bare potential, much as would be expected if the electrons were noninteracting, but the Coulomb repulsion causes the edges of these areas to spread out to

form metallic rings. Close to one-half filling fraction, these rings join to form a percolating metallic region, which is present over a range of filling fraction until the full regions percolate.

For typical Hall samples, both regimes arise, with a crossover from interaction dominated at high magnetic field, when the electrons occupy only low Landau levels, to potential dominated at lower magnetic field, when the electrons fill higher Landau levels. In both regimes there is a transition from a percolating empty region (electrons
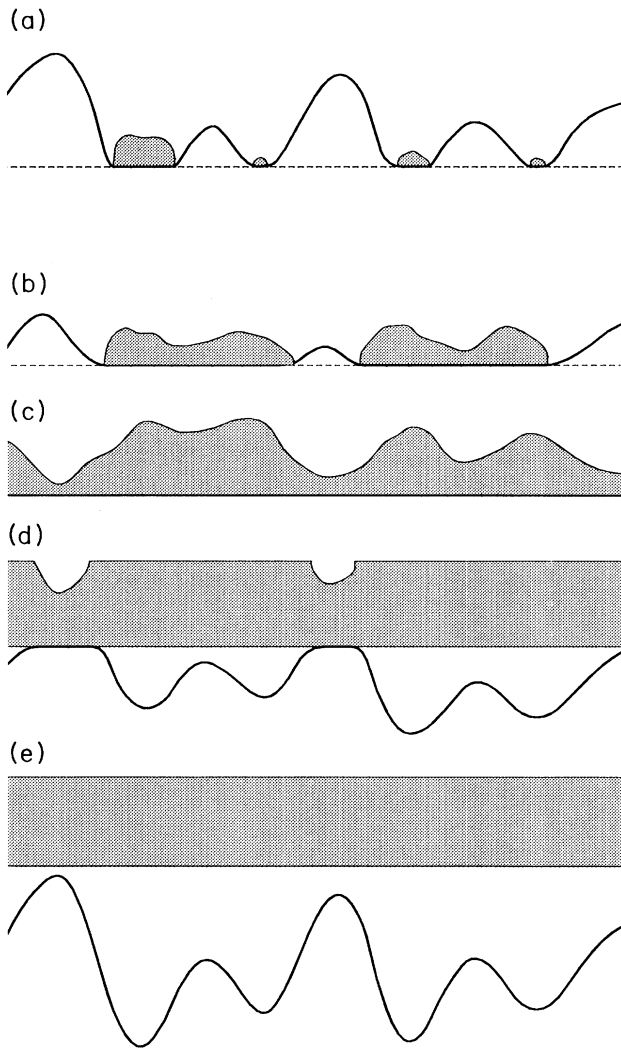


FIG. 1. The electron density distribution (shaded region) and screened potential (solid line) as the filling fraction of the partially occupied Landau level increases from 0 to 1 in the interaction-dominated regime: (a) At first, the electrons sit as metallic regions in the wells of the potential; (b) these grow to form a percolating metallic region around localized empty regions; (c) over a range of filling fraction, the metallic region covers the sample, giving perfect screening; (d) full regions appear, which grow in size and percolate, leaving localized metallic regions; and (e) eventually, the full regions cover the sample and the bare potential is unscreened.
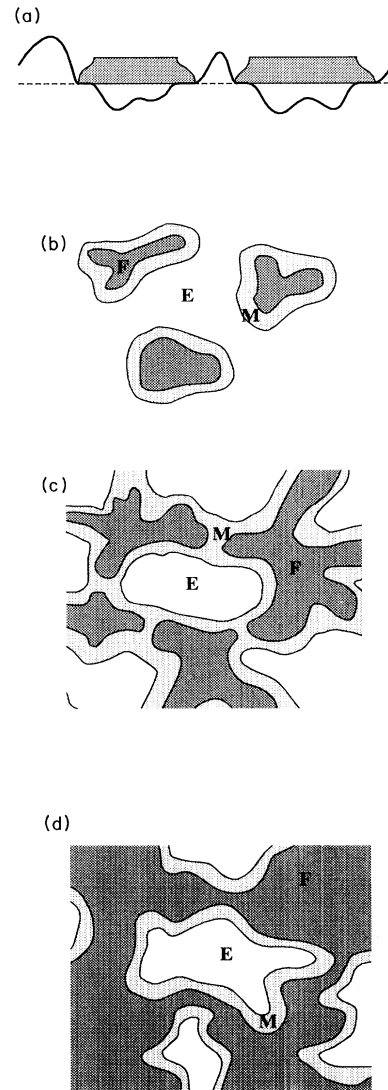


FIG. 2. Screening in the potential-dominated regime: (a) The electrons form full regions in the minima of the bare potential with narrow metallic regions at their boundaries. When viewed from above, it can be seen that, as the average filling factor increases, the screening distribution changes character from (b) percolating empty to (c) percolating metallic and, finally, to (d) percolating full. Areas in which the Landau level is locally empty, partially occupied ("metallic"), and full are denoted by E, M, and F, respectively.

localized), to a percolating metallic region which lasts over a range of filling fractions, and finally to a percolating full region. It is the percolating metallic region that we will show to be associated with dissipative behavior and steps between Hall plateaus. We note finally that this screening theory breaks down in low magnetic field, when the width of the metallic regions is no longer much greater than the diameter of a cyclotron orbit in the highest occupied Landau level.

### C. Quantitative analysis

In Sec. V E we shall focus on behavior in the potential-dominated regime, in which the metallic regions occupy a small fraction of the sample. It is of interest to know how the density varies across the metallic regions. The mathematical difficulties associated with the solution of the self-consistent pair of equations limit analytic work to simplified geometries. We consider a strip of electrons in the $x$-$y$ plane, held in a confining potential which varies only in the $x$ direction, with a constant gradient at one edge and an infinite step at the other. This creates a metallic region at one edge and a sharp

boundary between full and empty at the other.

Following the approach used by Chklovskii, Shklovskii, and Glazman,[23] we solve a two-dimensional electrostatics problem (in the $x$-$z$ plane, perpendicular to the strip of charge) with boundary conditions on the line $z = 0$,

$$n(x) = \begin{cases} 0, & x < -w_M/2; x > w_F + w_M/2 \\ & \text{(empty regions)} \\ n_0, & w_M/2 < x < w_F + w_M/2 \quad \text{(full region)} , \end{cases} \qquad (3.4)$$

$$\frac{\partial W}{\partial x} = \alpha , \quad -w_M/2 < x < w_M/2 \quad \text{(metallic region)} ,$$

$$(3.5)$$

for the electrostatic potential energy $W(x,z)$, set up by the electron distribution, so that in the metallic region a bare potential of constant gradient $-\alpha$ is screened [Eq. (3.5)].

We find that the density distribution in the metallic edge, $-w_M/2 < x < w_M/2$, is

$$n(x) = \frac{2}{\pi} n_0 \left\{ \arctan\left[ \frac{w_F + w_M/2 - x + \sqrt{(w_F + w_M/2)^2 - w_F^2}}{\sqrt{(w_M/2)^2 - x^2}} \right] - \arctan\left[ \frac{w_M/2 - x}{w_M/2 + x} \right]^{1/2} \right\} . \qquad (3.6)$$

The boundary condition that $\partial W/\partial x \to 0$ for $|x| \to \infty$ requires

$$\alpha = \frac{n_0 e^2}{2\pi\epsilon\epsilon_0} \ln\left\{ \frac{2w_F}{w_M} + 1 + \left[ \left( \frac{2w_F}{w_M} + 1 \right)^2 - 1 \right]^{1/2} \right\} , \quad (3.7)$$

which fixes the ratio of the width of the metallic strip to the width of the full region, in terms of the bare potential gradient and the interaction strength.

For the potential-dominated regime, $w_M/w_F \to 0$, and Eq. (3.7) can be simplified to find

$$w_M = 4w_F \exp\left[ -\alpha \frac{2\pi\epsilon\epsilon_0}{n_0 e^2} \right] . \qquad (3.8)$$

Similarly, the density becomes

$$n_S(x) = \frac{n_0}{\pi} \arccos\left[ -\frac{2x}{w_M} \right] , \quad |x| < w_M/2 . \qquad (3.9)$$

Note that for $n_0 e^2/2\pi\epsilon\epsilon_0 > \alpha$, the size of the metallic region is comparable to the size of the full region and the system is in the interaction-dominated regime where the metallic regions are large. This provides a justification of the criterion for perfect screening quoted in Sec. III B.

## IV. NONEQUILIBRIUM ELECTRON FLOW AND TRANSMISSION COEFFICIENTS

### A. Introduction

To describe transport phenomena within this framework, it is necessary to extend the model to allow nonequilibrium distributions. The approximations used above (valid for $d \gg l$ and $\hbar\omega/l \gg \sqrt{\langle |\nabla W_B|^2 \rangle}$) allow the electron distribution to be represented by the electron number density $n(\mathbf{r}, t)$ and the electron motion by a number current density $\mathbf{j}(\mathbf{r}, t)$. At equilibrium, the number density is uniquely determined[12] and time independent, but in general any distribution may be specified, which will then evolve according to the flow equations

$$e\mathbf{j}(\mathbf{r}, t) = -\sigma[n(\mathbf{r}, t)] \cdot \nabla W(\mathbf{r}, t)/e , \qquad (4.1)$$

$$\frac{\partial n(\mathbf{r}, t)}{\partial t} = -\nabla \cdot \mathbf{j}(\mathbf{r}, t) , \qquad (4.2)$$

$$W(\mathbf{r}, t) = W_B(\mathbf{r}) + \int I(\mathbf{r} - \mathbf{r}') n(\mathbf{r}', t) d^2\mathbf{r}' . \qquad (4.3)$$

Thus we assume that currents flow in response to the total potential gradient according to a *local* conductivity tensor $\sigma(n)$. In the first instance, we ignore inelastic scattering, in which case the electrons travel at right angles to the field gradient:

$$\sigma(\mathbf{r},t)=n(\mathbf{r},t)\begin{bmatrix} 0 & -e/B \\ e/B & 0 \end{bmatrix}$$

$$=\frac{n(\mathbf{r},t)}{n_0}\begin{bmatrix} 0 & -\sigma_H \\ \sigma_H & 0 \end{bmatrix}, \tag{4.4}$$

with $\sigma_H=\pm e^2/h$, according to the sign of the magnetic field.

We shall look for time-independent solutions of the above equations, $\nabla\cdot\mathbf{j}=0$, which leads to the condition

$$(\nabla n\times\nabla W)_z=0 . \tag{4.5}$$

This requires that the potential gradient at any point be perpendicular to the density contour through the point, ensuring that currents flow along density contours and that the electron distribution and the potential are time independent.

Equation (4.5) is a general condition for steady-state distributions and makes no reference to the equilibrium state described in Sec. III. To make use of this equilibrium density distribution, we shall consider small changes away from it:

$$n(\mathbf{r})=n_S(\mathbf{r})+\delta n(\mathbf{r}) , \tag{4.6}$$

$$W(\mathbf{r})=W_S(\mathbf{r})+\delta W(\mathbf{r}) . \tag{4.7}$$

Since $W_S(\mathbf{r})$ is constant in a metallic region and $n_S(\mathbf{r})$ is constant in full and empty regions, the linearized form of (4.5) with respect to the small changes $\delta n(\mathbf{r})$ and $\delta W(\mathbf{r})$ becomes

$$(\nabla n_S\times\nabla\delta W)_z=0 \tag{4.8}$$

in metallic regions and

$$(\nabla\delta n\times\nabla W_S)_z=0 \tag{4.9}$$

in full and empty regions.

We shall see that any change of the charge density in an empty or a full region is confined to its boundary with the metallic region, where the screened field gradient falls to zero. As a result, (4.9) will always hold, and only (4.8) will restrict the potential $\delta W(\mathbf{r})$.

### B. Linear response of a single saddle point in the equilibrium density

The Landauer-Büttiker approach to conductance calculations[16] regards currents as the driving force and determines potentials from the charge redistribution due to elastic scattering in the sample. We are now ready to apply this approach to the linear response of the equilibrium screening distribution described in Sec. III.

Consider a bare potential which consists of a single saddle point and has the screening density shown in Fig. 3(a), where the contours indicate the local filling fraction $v(\mathbf{r})=n(\mathbf{r})/n_0$. We shall assume for the present that this is the only Landau level occupied, and later introduce the lower levels. At equilibrium the metallic region carries no current, as the screened potential there is constant, but the full regions carry circulating diamagnetic currents along the contours of the screened potential. For a po-
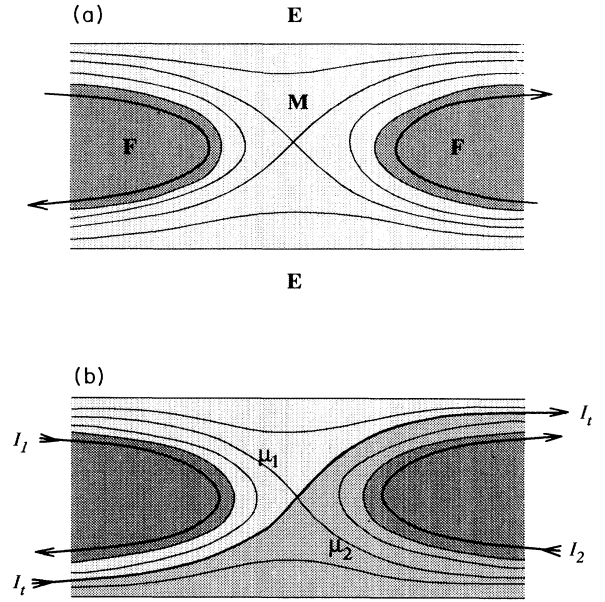


FIG. 3. (a) Electron distribution near a single saddle point in the equilibrium density. Arrows indicate the flow of diamagnetic currents. E, M, and F denote empty, metallic, and full regions. (b) When the potentials at the inputs are raised to $\mu_1$ and $\mu_2$, the potential difference falls as a sharp step along the density contour crossing the saddle point; arrows indicate the additional current flow. A current $I_t=v_s\sigma_H(\mu_1-\mu_2)/e$ crosses the saddle point from channel 4 to channel 3.

tential gradient of $|\nabla W_S|$, there is a perpendicular local current density [see Eqs. (4.1) and (4.4)] along the equipotentials, of size $\sigma_H|\nabla W_S|/e$, where $\sigma_H$ is the Hall conductance for a single full Landau level and is independent of the magnetic-field strength. For definiteness, from here on we shall assume that the direction of the magnetic field is such that $\sigma_H$ is a positive quantity. The arrows in Fig. 3(a) indicate the directions of current flow and serve to identify the channels marked 1 and 2 as inputs and 3 and 4 as outputs.

In the spirit of the Landauer-Büttiker approach, we consider connecting the input channels to ideal reservoirs at chemical potentials $\mu_1$ and $\mu_2$, which fixes the input currents. Due to elastic scattering in the bulk of the sample, we expect to find nonequilibrium distributions of electrons in the outgoing channels. Inelastic processes in the leads from these channels relax the distributions to local equilibrium at some intermediate values of chemical potential. In this way the current and chemical potentials of each channel are determined, and the conductance of the system is fully defined.

Local equilibrium of channel 1 at a (small) chemical potential $\mu_1$ (relative to the Fermi level) means that the metallic region of that channel lies in a uniform potential of $\mu_1$. In linear response, the current in the adjacent full region is increased by $\sigma_H\mu_1/e$. Similarly, the potential $\mu_2$ injects an additional current $\sigma_H\mu_2/e$ through channel 2. The microscopic model must now provide a way of con-

necting these two channels with a steady-state potential distribution and hence specify the current distribution in the outgoing channels. The condition under linear response for a steady state, Eq. (4.8), requires that the field gradient, which must somehow occur in the metallic region of the saddle point, is restricted to be perpendicular to a contour of the equilibrium screening density. The only way to achieve this is to have a sharp step in the potential from $\mu_1$ to $\mu_2$ along the density contour which crosses the saddle point, as indicated by the shading in Fig. 3(b). A similar conclusion has been reached independently by Chklovskii, Matveev, and Shklovskii,[18] following a different approach.

To generate this step, there is a redistribution of electrons, $\delta n(\mathbf{r})$, which is required to satisfy (4.9) and is further restricted to be negative in full regions and positive in empty regions. To find this distribution, imagine calculating the equilibrium screening distribution for a potential which is $W_B(\mathbf{r}) - \delta W(\mathbf{r})$ in the metallic regions [and arbitrary but close to $W_B(\mathbf{r})$ in the full and empty regions]. For small enough $\delta W(\mathbf{r})$, this distribution will be similar to $n_S(\mathbf{r})$, with the boundaries of full, empty, and metallic regions slightly displaced. If this distribution is placed in a bare potential $W_B(\mathbf{r})$, there is a resultant potential $\delta W(\mathbf{r})$ in the metallic regions which satisfies (4.8). The changes of density in full or empty regions are confined to their edges where $\nabla W_S \to 0$ and (4.9) is satisfied. This distribution is therefore the required $n_S(\mathbf{r}) + \delta n(\mathbf{r})$, demonstrating that a small step $\delta W(\mathbf{r})$ can always be generated.

The potential step occurs in a region where the filling fraction is that of the percolating contour of the equilibrium density $v_s$, and causes a current $I_t = v_s \sigma_H(\mu_1 - \mu_2)/e$ to flow from lead 4 to lead 3. The currents in each of the channels are, therefore,

$$I_1 = \sigma_H \mu_1/e ,$$
$$I_2 = \sigma_H \mu_2/e ,$$
$$I_3 = \sigma_H \mu_2/e + v_s \sigma_H(\mu_1 - \mu_2)/e = v_s I_1 + (1 - v_s)I_2 ,$$
$$I_4 = \sigma_H \mu_1/e - v_s \sigma_H(\mu_1 - \mu_2)/e = (1 - v_s)I_1 + v_s I_2 .$$

$$(4.10)$$

Channels 3 and 4 are clearly not in local equilibrium, so at present do not have well-defined chemical potentials. In order to associate a chemical potential with each of these channels, inelastic processes are assumed to occur far from the saddle point. These relax the density distribution in each to a local equilibrium, in which each metallic region is at a constant potential and all current flows in the full regions. Using current conservation in each channel, the chemical potentials of the output leads must be

$$\mu_3 = \mu_2 + v_s(\mu_1 - \mu_2) ,$$
$$\mu_4 = \mu_1 - v_s(\mu_1 - \mu_2) .$$

$$(4.11)$$

The conductance of the system is now implicitly determined. We discuss its behavior below.

## C. Transmission coefficients and the conductance

The results of Sec. IV B may be conveniently reexpressed in the language of transmission coefficients. Following Streda, Kucera, and MacDonald,[25] transport in this four-terminal device may be described by the transmission and reflection probabilities $T$ and $R$ of the single occupied level. These are defined, respectively, as the probability for an electron incident in channel 1 (channel 2) to leave through channel 3 (channel 4) and the probability of reflection from channel 1 (2) into 4 (3). Current conservation requires $R = 1 - T$, so that the four-terminal device is characterized by a single parameter $T$. From Eq. (4.10), we can immediately write

$$T = 1 - R = v_s ,$$

$$(4.12)$$

where $v_s$ is the filling fraction on the density contour that crosses the saddle point.

For this one Landau-level device, the longitudinal and Hall resistances are found to be[25]

$$R_L \equiv \frac{\mu_1 - \mu_3}{e(I_1 - I_4)} = \frac{h}{e^2} \frac{R}{T} = \frac{h}{e^2} \frac{(1 - v_s)}{v_s} ,$$

$$(4.13)$$

$$R_H \equiv \frac{\mu_1 - \mu_4}{e(I_1 - I_4)} = \frac{h}{e^2} .$$

$$(4.14)$$

The longitudinal resistance behaves as expected: $R_L = 0$ when $v_s = 1$ and the saddle point is covered by full region (quantum Hall plateau); $R_L$ rises as $v_s$ decreases, to diverge when $v_s = 0$ and the two sides are disconnected. The Hall resistance is necessarily always quantized for this device, as it is measured across a portion of the system where current flows in a fully occupied region. Model devices with separate current and voltage contacts (Sec. V) do not share this behavior.

## D. Transport in the presence of dissipation

So far, we have assumed that electron motion in the bulk of the device is ideal, in the sense that it is described by a purely off-diagonal, local conductivity (4.4). Inelastic scattering was assumed to be present only in the leads to the device, and was necessary to relax the distribution to local equilibrium. This led to the conclusion that a simple model device supports a sharp step in the chemical potential when driven out of equilibrium. It is not clear whether such a potential distribution is stable against the presence of a small amount of inelastic scattering in the bulk of the device, represented by a small diagonal component in the local conductivity tensor (4.4). Such dissipation could arise, for example, from scattering by acoustic phonons. It is the purpose of the rest of this section to show that the results do remain valid, provided inelastic scattering is not too strong. Similar questions have been investigated recently for different geometries by Ruzin.[19]

More generally, the electron flow should be described in (4.1) by writing

$$\sigma[n(\mathbf{r})] = \begin{bmatrix} \sigma_{xx}[n(\mathbf{r})] & -\sigma_{xy}[n(\mathbf{r})] \\ \sigma_{xy}[n(\mathbf{r})] & \sigma_{xx}[n(\mathbf{r})] \end{bmatrix} ,$$

$$(4.15)$$

which includes a (positive) density-dependent diagonal conductivity $\sigma_{xx}[n(\mathbf{r})]$, due to inelastic scattering of the electrons. In a Drude theory, $\sigma_{xx}$ and $\sigma_{xy}$ are both simply proportional to $n(\mathbf{r})$ with a coefficient related to the inelastic scattering time $\tau$ (Ref. 26):

$$\sigma_{xx}(n)=\frac{\omega\tau}{1+(\omega\tau)^2}\frac{en}{B}\equiv\sigma_0\frac{n}{n_0}\simeq\frac{1}{\omega\tau}\frac{e^2}{h}\frac{n}{n_0} , \quad (4.16)$$

$$\sigma_{xy}(n)=\frac{(\omega\tau)^2}{1+(\omega\tau)^2}\frac{en}{B}\equiv\sigma_H\frac{n}{n_0}\simeq\frac{e^2}{h}\frac{n}{n_0} , \quad (4.17)$$

to first order in $1/\omega\tau$, where $\omega$ is the cyclotron frequency.

We expect this to be valid close to $n=0$. However, when $n$ is close to $n_0$, there are few empty final states for scattering and $\sigma_{xx}$ must decrease with increasing $n$, becoming zero at $n=n_0$, while $\sigma_{xy}$ is still given by $\sigma_H n/n_0$. Between these two extremes, $\sigma_{xx}(n)$ varies smoothly, and the conductivity tensor can be written as

$$\sigma=\begin{bmatrix} \sigma_{xx}(n) & -\sigma_H n/n_0 \\ \sigma_H n/n_0 & \sigma_{xx}(n) \end{bmatrix} , \quad (4.18)$$

where $\sigma_{xx}(n)$ falls to zero at $n\rightarrow0$ and $n\rightarrow n_0$.

With this form of conductivity, the (nonlinear) steady-state condition (4.5) becomes

$$\sigma_{xx}(n)\nabla^2 W+\nabla\sigma_{xx}(n)\cdot\nabla W-\frac{\sigma_H}{n_0}(\nabla n\times\nabla W)_z=0 . \quad (4.19)$$

Linearizing with respect to small deviations from the equilibrium distribution, Eqs. (4.6) and (4.7), gives

$$\sigma_{xx}(n_S)\nabla^2\delta W+\nabla\sigma_{xx}(n_S)\cdot\nabla\delta W-\frac{\sigma_H}{n_0}(\nabla n_S\times\nabla\delta W)_z=0 \quad (4.20)$$

in the metallic regions.

In the following, the ratio $\sigma_0/\sigma_H$ will be used as the small parameter which determines the strength of dissipation. From the discussion above, $\sigma_0/\sigma_H=1/\omega\tau$, which is much less than unity for well-defined Landau levels. Even if Drude theory is inappropriate, this ratio is still a measure of the local dissipation, and will be small if inelastic scattering is not to destroy the Landau bands.

### E. Effect of dissipation on transport across a saddle point in the equilibrium density

Near a saddle point in the equilibrium electron density, the density distribution varies as

$$n_S(x,y)=n_s+n_0\frac{xy}{l_s^2} , \quad (4.21)$$

where $n_s$ is the density of the contour which crosses the saddle point and $l_s$ is the length scale on which the density varies. Linearizing the variations in the diagonal conductivity with respect to the small changes in $n_S$ near the origin gives

$$\sigma_{xx}(x,y)=\sigma^0+\sigma'\frac{xy}{l_s^2} , \quad (4.22)$$

where $\sigma^0$ and $\sigma'$ depend on $n_s$, but lie in the ranges $0\le\sigma^0\le\sigma_0$, $-\sigma_0\le\sigma'\le\sigma_0$. For this situation, Eq. (4.20) becomes

$$\sigma^0\nabla^2\delta W+\frac{\sigma'}{l_s^2}\left[y\frac{\partial\delta W}{\partial x}+x\frac{\partial\delta W}{\partial y}\right]$$
$$-\frac{\sigma_H}{l_s^2}\left[y\frac{\partial\delta W}{\partial y}-x\frac{\partial\delta W}{\partial x}\right]=0 . \quad (4.23)$$

We now rotate to new coordinates,

$$\xi\propto x+[\sqrt{1+(\sigma_H/\sigma')^2}-(\sigma_H/\sigma')]y$$
$$\phi\propto-[\sqrt{1+(\sigma_H/\sigma')^2}-(\sigma_H/\sigma')]x+y , \quad (4.24)$$

so that the $\xi$ ($\phi$) axis lies at a (small) angle $\psi$ to the $x$ ($y$) axis, with

$$\psi=\arctan[\sqrt{1+(\sigma_H/\sigma')^2}-(\sigma_H/\sigma')]\simeq\frac{1}{2}\frac{\sigma'}{\sigma_H} . \quad (4.25)$$

With this change of variables, $\delta W(\xi,\phi)$ satisfies

$$\sigma^0\nabla^2\delta W+\frac{\sqrt{\sigma'^2+\sigma_H^2}}{l_s^2}\left[\xi\frac{\partial\delta W}{\partial\xi}-\phi\frac{\partial\delta W}{\partial\phi}\right]=0 , \quad (4.26)$$

which allows solution by the separation $\delta W(\xi,\phi)=\Xi(\xi)\Phi(\phi)$.

As boundary conditions, we require that the potential tend to constant values far from the origin (in the regions of local equilibrium). The only solution of (4.26) is then

$$\frac{d\Xi}{d\xi}=A\exp\left[-\frac{1}{2}\frac{\sqrt{\sigma'^2+\sigma_H^2}}{\sigma^0 l_s^2}\xi^2\right] , \quad (4.27)$$

$$\frac{d\Phi}{d\phi}=0 . \quad (4.28)$$

This represents an error function step in $\delta W$ of width

$$[(\sigma^0)^2/(\sigma'^2+\sigma_H^2)]^{1/4}l_s\simeq\sqrt{\sigma^0/\sigma_H}l_s ,$$

at a small angle $\psi$ to the density contour. The width of the step increases with $\sigma^0$, but provided

$$\sigma^0/\sigma_H\sim\sigma_0/\sigma_H=1/\omega\tau\ll1 ,$$

it is much narrower than the length scale on which the density changes. For a smooth saddle-point density distribution, therefore, inelastic scattering does not affect the qualitative feature that the chemical potential falls in a narrow step along a contour of filling fraction $\nu_s=n_s/n_0$. The nonequilibrium current flow from lead 4 to lead 3 is still $I_t=\nu_s\sigma_H(\mu_1-\mu_2)/e$, so the transmission coefficient of the device remains equal to $\nu_s$.

## F. Equilibration of the output channels

We next address the question of how a nonequilibrium potential distribution relaxes in the output channels. Consider the case of an edge channel which is translationally invariant in the $y$ direction, with $n(x)=0$ for $x < -w_M/2$ and $n(x)=n_0$ for $x > w_M/2$. The steady-state equation (4.20) becomes

$$\frac{\partial}{\partial x}\left[\sigma_{xx}(x)\frac{\partial \delta W}{\partial x}\right] - \frac{\sigma_H}{n_0}\frac{dn_S}{dx}\frac{\partial \delta W}{\partial y} = 0 \ , \qquad (4.29)$$

where we have neglected the second derivative with respect to $y$, which we expect to be small for $\sigma_0/\sigma_H \ll 1$.

This can be separated by writing $\delta W(x,y)=X(x)Y(y)$ to obtain the pair of equations,

$$\frac{d}{dx}\left[\sigma_{xx}(x)\frac{dX}{dx}\right] + \kappa\frac{\sigma_H}{n_0}\frac{dn_S}{dx}X = 0 \ , \qquad (4.30)$$

$$\frac{dY}{dy} + \kappa Y = 0 \ . \qquad (4.31)$$

The requirement that $\nabla\cdot\mathbf{j}=0$ leads to the boundary condition

$$\sigma_{xx}(x)\frac{\partial \delta W}{\partial x}\bigg|_{x=\pm w_M/2} = 0 \ . \qquad (4.32)$$

Equation (4.30) is an eigenfunction equation with a Hermitian operator for the space of functions on $|x|\le w_M/2$ which satisfy (4.32). The eigenfunctions of such an operator, $X_i(x)$, form an orthonormal basis for the space with respect to the inner product

$$\int_{-w_M/2}^{w_M/2}\frac{dn_S}{dx}X_i(x)X_j(x)dx = \delta_{ij} \ , \qquad (4.33)$$

where we assume $dn_S/dx > 0$ for $|x|\le w_M/2$.

The input to the channel is the potential distribution $\delta W(x,0)$, which in the case of interest is a narrow step. This may be expressed as a sum over the eigenfunctions

$$\delta W(x,0) = \sum_m a_m X_m(x) \ , \qquad (4.34)$$

$$a_m = \int_{-w_M/2}^{w_M/2}\frac{dn_S}{dx}\delta W(x,0)X_m(x)dx \ . \qquad (4.35)$$

The $y$ dependence is $Y_{\kappa_m}(y)\propto\exp(-\kappa_m y)$, so we obtain the full solution:

$$\delta W(x,y) = \sum_m a_m X_m(x)e^{-\kappa_m y} \ . \qquad (4.36)$$

Since $\sigma_{xx}(x)\ge 0$ on $|x|\le w_M/2$, the (discrete) eigenvalues $\kappa_m\sigma_H/n_0$ are positive semidefinite and all eigenmodes with $\kappa_m\ne 0$ are exponentially damped in the positive $y$ direction (the "output" direction). Note that from dimensional arguments, $\kappa_m\propto(\sigma_0/\sigma_H)1/w_M$, so that $\partial^2/\partial y^2\propto\kappa_m^2$ is negligible compared to the other terms due to the smallness of $\sigma_0/\sigma_H$, justifying our neglect of it earlier.

After a distance

$$\Delta y > 1/\kappa_1 \propto (\sigma_H/\sigma_0)w_M \ ,$$

where $\kappa_1$ is obtained from the eigenvalue of the first excited state, the potential has decayed to $\delta W(x,\infty) = a_0X_0(x)$. For all $\sigma_{xx}(x)$ and $n_S(x)$, the eigenfunction associated with the eigenvalue zero, $X_0(x)$, is simply a constant, and we find

$$\delta W(x,\infty) = \delta W(w_M/2,0) + \int_{-w_M/2}^{w_M/2}e^2\frac{j_y(x,0)}{\sigma_H}$$

$$+ \frac{\sigma_{xx}(x)}{\sigma_H}\frac{\partial \delta W(x,0)}{\partial y}dx$$

$$\simeq \delta W(w_M/2,0) + \frac{e}{\sigma_H}I_y \ , \qquad (4.37)$$

where the approximation in (4.37) neglects a second-order term in $\sigma_0/\sigma_H$.

This shows that the potential distribution decays to a constant potential at such a value that the excess current $I_y$, which was flowing in the $y$ direction in the metallic edge at $y=0$, all flows in the full region as $y\to\infty$. An approximation was necessary in the final step of Eq. (4.37) due to our earlier neglect of the $\partial^2/\partial y^2$ term in (4.20), with the result that current is conserved only to first order in $\sigma_0/\sigma_H$.

Although this final conclusion does not depend on the shape of the edge distribution or the specific form of the diagonal conductivity, it is of interest to solve the problem in a particular case to obtain quantitative length scales for decay. We assume that $n_S(x)$ has the form given in Eq. (3.9). A reasonable choice for the diagonal conductivity is

$$\sigma_{xx}(n) = \frac{\sigma_0}{\pi}\sin\left[\frac{\pi}{n_0}n\right] \ , \qquad (4.38)$$

which ensures that, if the Landau level is, respectively, close to empty or full, the scattering rate is proportional to the density of electrons or holes, as discussed at the start of this section. In this case,

$$\sigma_{xx}(x) = \frac{2\sigma_0}{\pi w_M}\sqrt{(w_M/2)^2 - x^2} \ , \qquad (4.39)$$

and the eigenfunction equation (4.30) may be written

$$\frac{d}{dz}\left[\sqrt{1-z^2}\frac{dX_m}{dz}\right] + m^2\frac{1}{\sqrt{1-z^2}}X_m = 0 \ , \qquad (4.40)$$

where we have introduced the dimensionless variables, $z=2x/w_M$, and $m^2=\kappa_m(\sigma_H/\sigma_0)w_M/2$.

This is easily solved by making the change of variable, $z=\cos\theta$, to obtain the eigenfunctions

$$X_m(x) \propto \cos[m\ \arccos(2x/w_m)] \ ,$$

$$\kappa_m = (\sigma_0/\sigma_H)(2/w_M)m^2 \ , \qquad (4.41)$$

where $m$ is an integer, which are the type-I Chebyshev polynomials of order $m$.

It is now straightforward to find the full evolution of any potential, though we are primarily concerned with

the equilibration length. As the first excited state has eigenvalue $\kappa_1 = (\sigma_0/\sigma_H)(2/w_M)$, then after a distance $\Delta y = (\sigma_H/\sigma_0)(w_M/2)$, all modes above the zero mode have decayed and the potential is effectively constant.

This completes the analysis of the dissipative flow equations for a device with a single saddle point in its equilibrium electron density. Since the potential still falls as a sharp step in the bulk of the system, the results of the Landauer-Büttiker approach remain valid in the presence of a small amount of dissipation. Furthermore, the presence of a diagonal component in the local conductivity tensor explicitly causes equilibration in the output channels, and we no longer require the separate assumption of dissipation in the leads. Inclusion of a diagonal component in the flow equations provides a complete phenomenological theory of transport in the Landau level.

## V. CONDUCTANCE OF HALL BARS

### A. Introduction

In Sec. IV we have presented a theory for electron transport in a single Landau level and have used it to describe a simple device. In the following we apply these ideas to more realistic Hall-bar geometries, which have separate voltage and current contacts, are much larger than the length scale of disorder, and have many Landau levels occupied.

Two simple limits arise. First, for samples much smaller than a *dissipation length* (defined below), the effect of inelastic scattering is negligible: The potential difference falls in sharp steps along contours of the equilibrium screening distribution, in the manner of the single saddle-point device discussed in Sec. IV. The longitudinal resistance is almost zero. The Hall resistance measured between voltage contacts has a value related to the density of the percolating contour, and is not quantized when a metallic region percolates the sample. Second, for samples much larger than the dissipation length, transport in the partially occupied level can be characterized by a resistivity. Then, when a metallic region percolates, the Hall resistance is not quantized, and the longitudinal resistance is nonzero. We show in particular that, in the potential-dominated regime, this resistivity depends only on the equilibrium density distribution and is independent of the strength of local dissipation, over a range of values of $\sigma_0/\sigma_H$.

### B. Conductance calculations and the quantum Hall effect

Consider a conventional Hall bar, in which a current is passed between two current contacts while voltage measurements are made across and along the device at separate contacts which draw no current. Figure 4(a) shows a screening density distribution for the partially occupied level of such a device in the interaction-dominated regime, with ideal leads attached to the sample, in such a way that in each lead there is always a full region which can support a current without dissipation.

In general, $N$ (spin-split) Landau levels will be (fully or

partially) occupied in the bulk of the sample. When the disorder is not strong enough to cause Landau bands to overlap, the $(N-1)$ lower bands are full in the bulk of the system and have density distributions of the form shown in Fig. 4(b), with a metallic edge where the density falls to zero (the "edge channel" of that layer). The edge channels of the different Landau levels are spatially separated (with the lowest level extending the furthest out), causing equilibration between Landau levels to be suppressed.[27] Experiments on selective population of the different levels[28,29] show that in high-mobility samples, the partially occupied level can remain in disequilibrium with the other levels. This has been explained by Chklovskii, Shklovskii, and Glazman[23] within the screening theory described in Sec. III. They have calculated the positions and widths of the edge channels for a particular
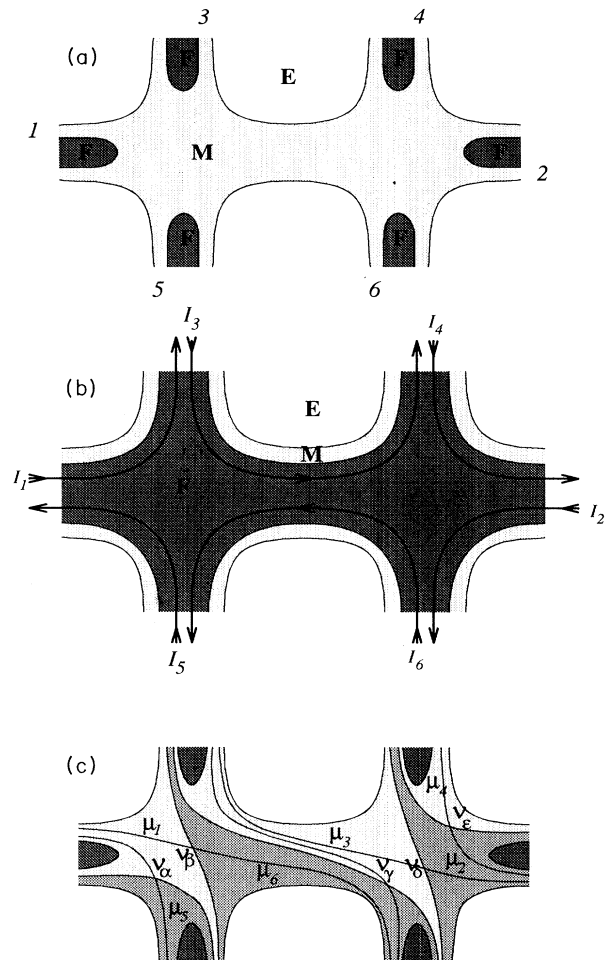


FIG. 4. (a) Equilibrium electron distribution in the partially occupied level of a Hall bar, in the interaction-dominated regime. The six terminals are attached to ideal leads. (b) The electron distribution for a full Landau level; the nonequilibrium current flows without backscattering. (c) When the inputs of the partially occupied level are held at $\mu_1, \mu_2, \ldots, \mu_6$, the potential falls in sharp steps crossing saddle-point contours; shading indicates the regions of constant potential.

confining potential and shown that the spatial separation of the partially occupied level from the edge channels of the other levels is so large that it is effectively decoupled. It is consistent with the screening theory for these devices, therefore, to treat electron flow in this highest level independently of the lower levels.

We now follow Büttiker[16] and use transport theory to calculate the currents which flow (independently) in each of the $N$ levels when contacts $1, 2, \ldots, 6$ are attached to particle reservoirs at chemical potentials $\mu_1, \mu_2, \ldots, \mu_6$. This imposes local equilibrium on the *input* side of each ideal lead and causes a transport current of $I_i^{\text{in}} = \sigma_H \mu_i / e$ to flow into the device through contact $i$ (in each Landau level) in addition to the equilibrium diamagnetic current. The output currents in each lead are determined by scattering in the sample. The requirement that the four voltage contacts (3, 4, 5, and 6) draw no net current leaves only two of the potentials arbitrary ($\mu_1$ and $\mu_2$, say). One of these sets the zero of energy, while the other fixes the overall current $I$. As a result, the potential difference between any pair of contacts is determined only by the current $I$, and the conductance of the sample is known.

The problem, therefore, is to find the output currents in each Landau level for a set of chemical potentials $\mu_1, \mu_2, \ldots, \mu_6$. This is straightforward for the $(N-1)$ full Landau levels in which there is no backscattering, and currents flow around the edge of the sample in a clockwise direction (with our choice of sign for $\sigma_H$), as indicated in Fig. 4(b). The output currents in each of these full Landau levels are simply given by[16]

$$I_1^{\text{out}} = I_5^{\text{in}} = \sigma_H \mu_5 / e \; ,$$

$$I_2^{\text{out}} = I_4^{\text{in}} = \sigma_H \mu_4 / e \; ,$$

$$I_3^{\text{out}} = I_1^{\text{in}} = \sigma_H \mu_1 / e \; ,$$

$$I_4^{\text{out}} = I_3^{\text{in}} = \sigma_H \mu_3 / e \; ,   \quad (5.1)$$

$$I_5^{\text{out}} = I_6^{\text{in}} = \sigma_H \mu_6 / e \; ,$$

$$I_6^{\text{out}} = I_2^{\text{in}} = \sigma_H \mu_2 / e \; .$$

Note that the edge channels of these Landau levels are always in local equilibrium with each other, so that it is unnecessary to restrict the rate of equilibration between them in order to consider them as effectively independent.

Next consider the transmission behavior of the $N$th level. If it has a percolating full region, then it behaves in the same way as the other Landau levels (5.1), and the restriction that 3 to 6 are voltage probes leads to $\mu_1 = \mu_3 = \mu_4$, $\mu_5 = \mu_6 = \mu_2$, and $I = N \sigma_H (\mu_3 - \mu_5)/e$. There is no longitudinal resistance drop, and the Hall resistance is in the $N$th quantum Hall plateau. Similarly, if the $N$th level has a percolating empty region, so that all probes are disconnected for this level, then no net currents flow in it ($I_i^{\text{out}} = I_i^{\text{in}}$), and the device shows a plateau for $(N-1)$ levels.

This argument simply establishes quantization of the Hall conductivity as a consequence of there being no backscattering[16] (or complete backscattering) of the elec-

trons in each level. The important feature of the present theory is that between these two extremes, the $N$th level has a percolating metallic region. The remainder of this paper addresses the determination of transmission properties of the percolating metallic region within various regimes. We demonstrate that risers between Hall plateaus have a finite width (in filling fraction) and in certain cases are accompanied by a corresponding peak in the longitudinal resistance.

## C. Transmission coefficients and conductance without local dissipation

We showed in Sec. III that the equilibrium screening distribution has two distinct regimes: interaction dominated and potential dominated. The dissipationless behavior of both of these regimes is the same and depends only on the densities corresponding to certain saddle points of the screening distribution.

Consider the density distribution in a sample with six ideal leads attached. Each probe must have a density contour which connects to another probe through a saddle point. In general, the contours between different pairs of probes will have different densities, which leaves five possible ways of connecting the probes together. Figure 4(c) shows (schematically) the relevant contours for one particular way this can occur. This is the case we shall consider in detail, but we will show that the other ways lead to the same results.

When the local conductivity of the metallic region is purely off diagonal, the steady-state condition under linear response (4.8) requires that any potential gradient must be perpendicular to a contour of the screening density. In Sec. IV we demonstrated that for a single saddle point, this requires a sharp step in the potential along the percolating contour. In the same way, Fig. 4(c) can be divided into regions of different chemical potential separated by sharp boundaries which cross the five saddle points. The output currents in the partially occupied layer are then

$$I_1^{\text{out}} = \sigma_H [\mu_1 + \nu_\alpha (\mu_5 - \mu_1)]/e \; ,$$

$$I_2^{\text{out}} = \sigma_H [\mu_2 + \nu_\epsilon (\mu_4 - \mu_2)]/e \; ,$$

$$I_3^{\text{out}} = \sigma_H [\mu_3 + \nu_\beta (\mu_1 - \mu_6) + \nu_\gamma (\mu_6 - \mu_3)]/e \; ,$$

$$I_4^{\text{out}} = \sigma_H [\mu_4 + \nu_\delta (\mu_3 - \mu_2) + \nu_\epsilon (\mu_2 - \mu_4)]/e \; ,   \quad (5.2)$$

$$I_5^{\text{out}} = \sigma_H [\mu_5 + \nu_\beta (\mu_6 - \mu_1) + \nu_\alpha (\mu_1 - \mu_5)]/e \; ,$$

$$I_6^{\text{out}} = \sigma_H [\mu_6 + \nu_\delta (\mu_2 - \mu_3) + \nu_\gamma (\mu_3 - \mu_6)]/e \; ,$$

where the first term in each is due to the complete reflection of the input current in the full region and $\nu_\alpha, \nu_\beta, \ldots, \nu_\epsilon$ are the filling fractions of the saddle points marked in Fig. 4(c).

Each of the saddle-point contours must extend a macroscopic distance through the bulk of the device. For samples much larger than the scale of the disorder fluctuations, the filling fraction of each saddle point must be close to that of the percolating contour for an infinite-sized bulk region $\nu_p$, and (5.2) becomes

$$I_1^{\text{out}} \simeq \sigma_H[\mu_1 + \nu_p(\mu_5 - \mu_1)]/e \ ,$$

$$I_2^{\text{out}} \simeq \sigma_H[\mu_2 + \nu_p(\mu_4 - \mu_2)]/e \ ,$$

$$I_3^{\text{out}} \simeq \sigma_H[\mu_3 + \nu_p(\mu_1 - \mu_3)]/e \ ,$$

$$I_4^{\text{out}} \simeq \sigma_H[\mu_4 + \nu_p(\mu_3 - \mu_4)]/e \ , \qquad (5.3)$$

$$I_5^{\text{out}} \simeq \sigma_H[\mu_5 + \nu_p(\mu_6 - \mu_5)]/e \ ,$$

$$I_6^{\text{out}} \simeq \sigma_H[\mu_6 + \nu_p(\mu_2 - \mu_6)]/e \ .$$

It is this condition which leads to the equivalence of the five possible connectivities.

Combining the behavior of the $N$th level with the transport in the lower levels, (5.1) determines the conductance of the whole device. We find $\mu_1 = \mu_3 = \mu_4$ and $\mu_5 = \mu_6 = \mu_2$, with the longitudinal and Hall resistances given by

$$R_L \equiv \frac{(\mu_3 - \mu_4)}{eI} = 0 \ , \qquad (5.4)$$

$$R_H \equiv \frac{(\mu_3 - \mu_5)}{eI} = \frac{1}{(N - 1 + \nu_p)} \frac{h}{e^2} \ . \qquad (5.5)$$

The voltage drop driving the current occurs as a sharp step along a contour of density $\nu_p$ which passes from contact 1 to contact 2, giving zero longitudinal resistance and a Hall resistance corresponding to the electron density on this contour. The behavior of this dissipationless regime is fully specified by the density of the percolating contour of the infinite system, which is a property of the equilibrium screening distribution alone. The Hall conductance is not quantized over the range of filling fractions for which a metallic region percolates and $\nu_p$ is noninteger.

In deriving these results, inelastic scattering has been neglected. It was shown in Sec. IV that it is correct to do so for a device with a smooth screening density, provided $\sigma_0/\sigma_H \ll 1$. The only effect of a diagonal component to the local conductivity is to broaden the potential step slightly. In a large, disordered sample, the condition for the validity of the dissipationless results becomes more restrictive. Consider an interaction-dominated partially occupied level, for which the density distribution has a perfect screening modulation of amplitude $\Delta n_S$, which varies on a length scale $d$. For devices much larger than this disorder length scale, the percolating contours are highly convoluted paths (the perimeters of percolation clusters) which can come within a distance $\simeq d$ of themselves. The dissipationless theory requires a potential step of width less than $d$ to follow this contour through the system. Imagine trying to impose such a step in the potential. Treating the contour as a straight path, the diagonal component in the conductivity tensor causes the step to spread to a width $d$ over an arc length

$$\Delta l \propto (\sigma_H/\sigma_0)(\Delta n_S/n_0)d$$

(since $\Delta n_S/d$ is the typical number density gradient). Because the contour is actually the boundary of a percolation cluster, one expects the end-to-end distance to scale with arc length as $(\Delta l/d)^p d$ (where the value of the criti-

cal exponent $p$ may differ from that for the conventional percolation problem because of the long-range force involved, but must lie in the range $\frac{1}{2} < p < 1$). This determines the dissipation length,

$$l_{\text{diss}} = [(\sigma_H/\sigma_0)(\Delta n_S/n_0)]^p d \ ,$$

which is the maximum distance a sharp step in the potential can be sustained across an interaction-dominated sample. The results derived above are valid in samples smaller than this dissipation length.

### D. Consequences for transport of local dissipation

For samples larger than the dissipation length, variations in potential are spread over the whole of the device, according to the steady-state condition in the presence of inelastic scattering, Eq. (4.20). One expects that transport in the bulk of a partially occupied level should be described by a *resistivity* $\rho_{ij}^N$ on scales large compared with $l_{\text{diss}}$. In these circumstances, a transport model can be developed, which is similar to that proposed by McEuen *et al.* on empirical grounds,[17] but with $\rho_{ij}^N$ a function of microscopic parameters.

The central problem, then, is to calculate $\rho_{ij}^N$. There are several different regimes, according to the relative size of $l_{\text{diss}}$ and $d$, and according to whether the equilibrium density distribution is potential or interaction dominated. We consider only the simplest of these, in which $l_{\text{diss}} \ll d$ and the potential dominates.

### E. Transport in the potential-dominated regime

The potential-dominated electron density distribution near half-filling, as described in Sec. III, consists of localized full and empty regions, with rings of metallic region of width $w_M$ at their boundaries which connect to form a percolating metallic region. This width defines the length scale over which the density varies, and the path length for dissipative spreading is then of order $(\sigma_H/\sigma_0)w_M$. We shall treat the situation in which the distance $d$ between saddle points of the equilibrium density is much larger than the equilibration length $(\sigma_H/\sigma_0)w_M$, and complete equilibration occurs between saddle points. This condition will always be realized far enough into the potential-dominated regime (strong enough disorder or high enough Landau level) since $w_m/d \to 0$. Note, however, that (depending on the sample) the screening theory of Sec. III may break down before this occurs.

It was shown in Sec. IV that flow in the vicinity of a saddle point is unaffected by dissipation provided $\sigma_0/\sigma_H \ll 1$. If $w_M/d \ll \sigma_0/\sigma_H \ll 1$, there is complete equilibration between saddle points and the system may be represented by a network of ideal saddle points, with the outputs from one saddle point determining the potentials at the inputs of adjoining saddle points. Transport in a partially occupied level may now be studied by solving for the potentials at the nodes of the network, with the voltage characteristics of each saddle point determined by its filling fraction through Eqs. (4.11).

To demonstrate the behavior of this model, consider the array of saddle points shown in Fig. 5(a). The saddle
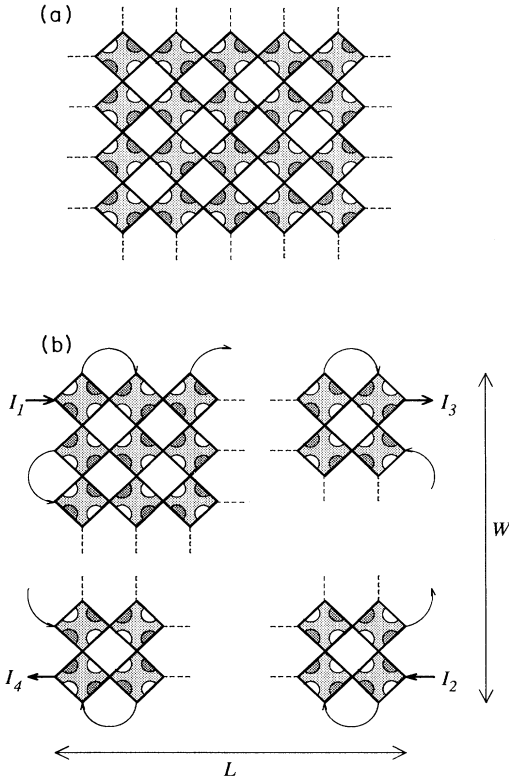
## (a)



## (b)



FIG. 5. (a) Translationally invariant square array of identical saddle points. A unit cell of the network contains two orientations of saddle points. (b) A four-terminal device may be constructed from this array by connecting adjacent nodes at the edges of a rectangular section.

points are assumed all to have the same filling fraction, so that the network is periodic with a unit cell which contains two saddle points (the two orientations). Because of translational invariance, a potential gradient $\mathbf{E}$ may be imposed across the network in such a way that the potential difference between nodes separated by a lattice vector $\mathbf{R}$ is $\mathbf{E} \cdot \mathbf{R}$. It is then straightforward to solve for the potential differences between nodes within a unit cell in terms of $\mathbf{E}$. The resultant net current is found to be related to the potential gradient by a conductivity

$$\sigma^N = \frac{e^2}{h} \frac{1}{v_s^2 + (1-v_s)^2} \begin{bmatrix} v_s(1-v_s) & -v_s^2 \\ v_s^2 & v_s(1-v_s) \end{bmatrix} , \quad (5.6)$$

where $v_s$ is the filling fraction of the unit saddle point. Thus $\sigma_{xx}^N$ is symmetric in filling factor about a maximum at $v_s = \frac{1}{2}$, and $\sigma_{xy}^N$ is antisymmetric about its value at $v_s = \frac{1}{2}$, varying from 0 to $e^2/h$ as $v_s$ increases from 0 to 1. Of course, over the ranges of *average* filling fraction for which the partially occupied level has a percolating empty or a percolating full religion, $v_s$ is strictly 0 or 1; it is only in the transition between these regimes that a metallic region percolates and $v_s$ is noninteger.

Inverting (5.6), we find that the resistivity of the array of Fig. 5(a) is

$$\rho^N = \frac{h}{e^2} \begin{bmatrix} \dfrac{1-v_s}{v_s} & 1 \\ -1 & \dfrac{1-v_s}{v_s} \end{bmatrix} . \quad (5.7)$$

Hence, the longitudinal and Hall resistivities of the array are simply equal to the longitudinal and Hall resistances of the unit saddle point.

One can also study current flow in a finite network. Consider a device made from a rectangular section of the square array. There are many inputs and outputs at the edges of the section; a confining potential will direct current from one to the next, leaving two inputs and two outputs at the four corners of the array [Fig. 5(b)]. Thus the two ends of the network are connected to ideal leads (as the voltage drop here only occurs across full regions), while the top and bottom edges represent boundaries with empty regions. In this case we find by explicit solution of the associated resistor network (after some algebra) that there are *no end or edge effects* associated with either the connections to the ideal leads or the boundaries to the empty regions. The network is characterized by a single resistivity, leading to the sample result that for *any size* of network of this type, the resistances (if only one Landau level is occupied) are

$$R_L^{\text{network}} = \frac{h}{e^2} \frac{1-T^{\text{network}}}{T^{\text{network}}} = \frac{L}{W} \frac{h}{e^2} \frac{1-v_s}{v_s} = \frac{L}{W} R_L , \quad (5.8)$$

$$R_H^{\text{network}} = \frac{h}{e^2} = R_H , \quad (5.9)$$

where $R_L$ and $R_H$ are the corresponding quantities for one of the saddle points and $L/W$ is the ratio of the number of saddle points in the length to the number in the width.

Finally, we consider samples in which more than one Landau level is occupied. If the partially occupied level remains in local equilibrium with the full Landau levels, the same electric field is felt by all levels. The conductivity of the device is then simply the sum of the conductivities of the $N$ levels.

If there is no such equilibrium, we need to distinguish voltage probes from current probes, as described earlier. To demonstrate how the conductance of a device varies with filling fraction, we follow ideas developed in the study of conduction by edge states,[17,30,31] and, for illustration, use the model introduced by McEuen et al., which divides the partially occupied layer into several sections (Fig. 6). In view of Eq. (5.8), each of the sections may be replaced by a single device with a longitudinal resistance determined by the filling fraction of the unit saddle point and the length-to-width ratio of the section. As before, transport in the partially occupied level is combined with that in the $(N-1)$ full levels, and it is required that probes 3 to 6 carry no net current. Figure 7 shows the variation in the Hall and longitudinal resistances of the device as a function of the filling fraction of
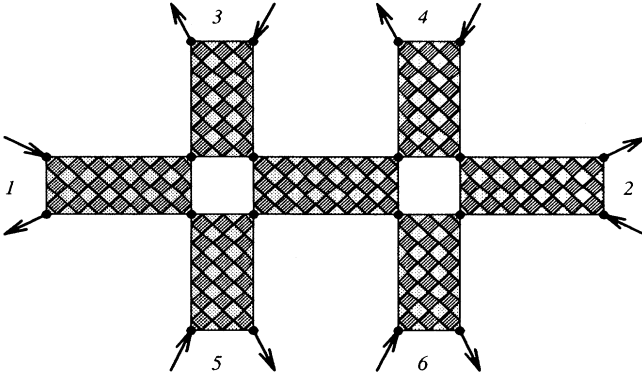
FIG. 6. The dissipative partially occupied level of the Hall bar may be represented by seven resistive sections.
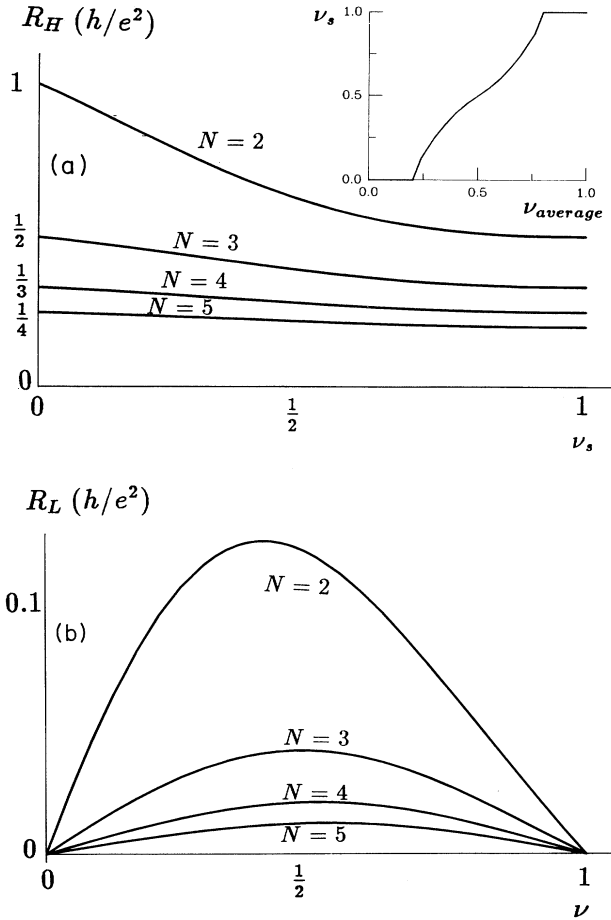


FIG. 7. Variation of (a) the Hall resistance and (b) the longitudinal resistance of a Hall bar with a partially occupied level represented by a saddle-point network. $N$ Landau levels are occupied and $v_s$ is the filling fraction of the saddle points of the partially occupied level. The inset to (a) schematically shows the variation of $v_s$ with average filling fraction: $v_s$ is equal to 0 over the range of average filling fraction for which an empty region percolates and equal to 1 when a full region percolates; between these plateau conditions, a metallic region percolates and $v_s$ sweeps from 0 to 1.

the saddle points of the partially occupied level, $v_s$, for the case in which all seven sections have a length-to-width ratio of unity.

When the highest Landau level has a percolating empty or full region, $v_s$ is 0 or 1, giving zero longitudinal resistance and a quantized Hall resistance; the device exhibits a quantum Hall plateau. Over the range of field for which a metallic region percolates, the filling fraction of the saddle points sweeps between 0 and 1, and the Hall resistance is not quantized. Thus, the Hall resistance steps between quantized plateaus over a finite range of filling fraction, with a simultaneous peak in the longitudinal resistance.

This qualitative behavior remains the same for all samples with a dissipative partially occupied level. Over the range of field for which a metallic region percolates, $\rho_{xx}^N$ is nonzero (necessarily, since dissipation is significant) with the consequence that the Hall resistance is not quantized and the longitudinal resistance is finite. Differences arise only in the detailed variation of $\rho_{ij}^N$ with average filling fraction, which affects the shape of the steps between quantized values, but not their width.

## VI. SUMMARY

Screening of a smoothly varying disordered potential in a strong magnetic field involves dramatic inhomogeneities in the charge density. There is a range of magnetic field over which a metallic region percolates in the partially occupied Landau level of the sample. We have presented a theory for transport including screening and have investigated the linear response of Hall samples under various regimes.

When the electrons suffer no inelastic scattering, we find that current flow is accompanied by a sharp step in the chemical potential within the sample, which follows a contour of the equilibrium density distribution. We have also studied transport in the presence of weak inelastic scattering and find that a sharp step in the potential remains in samples smaller than a dissipation length. The conductance of a small sample depends only on the filling fractions at saddle points of the density distribution. A Hall bar which is much larger than the disorder length scale, but smaller than a dissipation length, shows very small longitudinal resistance, and a Hall resistance which is related to the filling fraction of the percolating density contour, and is not quantized when a metallic region percolates.

In samples larger than the dissipation length, transport in the highest Landau level is characterized by a resistivity, which depends on microscopic parameters and leads to results resembling earlier empirical models. In the potential-dominated regime, where is a range of values for $\sigma_0/\sigma_H$ over which equilibration occurs between saddle points in the equilibrium density distribution. The resistivity can be calculated for a network of connected saddle points and depends on the equilibrium density distribution alone.

In all cases, over the range of filling fraction for which the equilibrium density distribution of the highest Landau level has a percolating metallic region, the Hall resistance is not quantized. For dissipative regimes there is a corresponding peak in the longitudinal resistance. This finite width for transitions between quantum Hall plateaus is a consequence of the electron-electron interactions and their effect on the low-temperature screening behavior.

[1]See *The Quantum Hall Effect*, edited by R. E. Prange and S. M. Girvin (Springer-Verlag, Heidelberg, 1990).
[2]M. Tsukada, J. Phys. Soc. Jpn. **41**, 1466 (1976); S. V. Iordansky, Solid State Commun. **43**, 1 (1982); R. F. Kararinov and S. Luryi, Phys. Rev. B **25**, 7626 (1982); S. A. Trugman, *ibid*. **27**, 7539 (1983); B. Shapiro, *ibid*. **33**, 8447 (1986).
[3]J. T. Chalker and P. D. Coddington, J. Phys. C **21**, 2665 (1988).
[4]H. P. Wei, D. C. Tsui, M. Paalanen, and A. M. M. Pruisken, Phys. Rev. Lett. **61**, 1294 (1988).
[5]H. P. Wei, S. Y. Lin, D. C. Tsui, and A. M. M. Pruisken, Phys. Rev. B **45**, 3926 (1992).
[6]S. Koch, R. J. Haug, K. von Klitzing, and K. Ploog, Phys. Rev. B **43**, 6828 (1991); Phys. Rev. Lett. **67**, 883 (1991).
[7]D. Heitman, M. Ziesmann, and L. L. Chang, Phys. Rev. B **34**, 7463 (1986).
[8]I. V. Kukushkin and V. B. Timofeev, Pis'ma Zh. Eksp. Teor. Fiz. **43**, 387 (1986) [JETP Lett. **43**, 499 (1986)].
[9]R. R. Gerhardts and V. Gudmundsson, Phys. Rev. B **34**, 2999 (1986).
[10]S. Luryi, in *High Magnetic Fields in Semiconductor Physics*, edited by G. Landwehr (Springer-Verlag, Heidelberg, 1987).
[11]S. Das Sarma and X. C. Xie, Phys. Rev. Lett. **61**, 738 (1988).
[12]A. L. Efros, Solid State Commun. **65**, 1281 (1988).
[13]A. L. Efros, Solid State Commun. **67**, 1019 (1988).
[14]A. L. Efros, Solid State Commun. **70**, 253 (1989).
[15]A. L. Efros, Phys. Rev. B **45**, 11 354 (1992).
[16]R. Landauer, IBM J. Res. Dev. **1**, 233 (1957); Philos. Mag. **21**, 836 (1970); M. Büttiker, Phys. Rev. B **38**, 9375 (1988).
[17]P. L. McEuen, A. Szafer, C. A. Richter, B. W. Alphenaar, J.

K. Jain, A. D. Stone, R. G. Wheeler, and R. N. Sacks, Phys. Rev. Lett. **64**, 2062 (1990).
[18]D. B. Chklovskii, K. A. Matveev, and B. I. Shklovskii, Phys. Rev. B **47**, 12 605 (1993).
[19]I. M. Ruzin (unpublished).
[20]J. Labbé, Phys. Rev. B **35**, 1373 (1987).
[21]U. Wulf, V. Gudmundsson, and R. R. Gerhardts, Phys. Rev. B **38**, 4218 (1988).
[22]D. Pfannkuche and J. Hajdu, Phys. Rev. B **46**, 7032 (1992).
[23]D. B. Chklovskii, B. I. Shklovskii, and L. I. Glazman, Phys. Rev. B **46**, 4026 (1992).
[24]H. Nielsen, Semicond. Sci. Technol. **5**, 604 (1990).
[25]P. Streda, J. Kucera, and A. H. MacDonald, Phys. Rev. Lett. **59**, 1973 (1987).
[26]N. W. Ashcroft and N. D. Mermin, *Solid State Physics* (Holt, Rinehart, and Winston, Orlando, Florida, 1976).
[27]G. Muller, D. Weiss, A. V. Khaetskii, K. von Klitzing, S. Koch, H. Nickel, W. Schlapp, and R. Lösch, Phys. Rev. B **45**, 3932 (1992).
[28]B. W. Alphenaar, P. L. McEuen, R. G. Wheeler, and R. N. Sacks, Phys. Rev. Lett. **64**, 677 (1990).
[29]B. J. van Wees, E. M. M. Willems, L. P. Kouwenhoven, C. J. Harmans, J. G. Williamson, C. T. Foxon, and J. H. Harris, Phys. Rev. B **39**, 8066 (1989).
[30]P. C. van Son, F. W de Vries, and T. M. Klapwijk, Phys. Rev. B **43**, 6724 (1991).
[31]S. Komiyama, H. Nii, M. Ohsawa, S. Fukatsu, Y. Shiraki, R. Ito, and H. Toyoshima, Solid State Commun. **80**, 157 (1991).